Access Point topology evaluation and optimization based on Cramér-Rao Lower Bound for WLAN indoor positioning

Elina Laitinen
Tampere University of Technology
Tampere, Finland
Email: elina.laitinen@tut.fi

Elena-Simona Lohan
Tampere University of Technology
Tampere, Finland
Email: elena-simona.lohan@tut.fi

Abstract—**WLAN Access Point network is typically optimized for communication scope, and not for localization. It is thus important to understand the positioning accuracy limits under a certain given Access Point topology and to be able to make design recommendations if the Access Point topology can be adapted better for the navigation needs. This paper calculates a Cramér-Rao Lower Bound -based criterion for Received Signal Strength -based positioning. Two study cases are presented about how the proposed criterion can be used to choose the optimal Access Point density and the optimal Access Point topology in a network designed for positioning purposes. In addition, our Cramér-Rao Lower Bound -based criterion can also be used to estimate the expected accuracy bound in an existing network, based on its underlying Access Point density or topology. Measurement -based results are used to verify our proposed approach.**

I. INTRODUCTION

Location-based Services (LBS) rely on accurate and available position information on Mobile Stations (MS). Since the Global Navigation Satellite Systems (GNSS) cannot offer user localization inside buildings due to multipaths, Non-Line-of-Sight (NLOS) and signal attenuation, [1], [2], other possible solutions are continuously searched. One widely researched approach, especially for indoor localization, is based on IEEE 802.11 standard [3] of Wireless Local Area Networks (WLAN/WiFi). The big advantage of WLAN-based positioning is economic efficiency, enabled by the availability in almost every device and the possibility to utilize the existing WLAN infrastructures.

Many WLAN-based positioning technologies are based on Received Signal Strength (RSS) measurements from Access Points (AP), see e.g. [4], [5]. One possible technique is database correlation, where the measured RSSs are tried to match with RSSs in a radiomap (fingerprinting method, FP). Another possibility is triangulation or trilateration based approach, where some path loss models are created and used to signal-to-distance mapping (path-loss estimation, PL). Since AP infrastructure is optimized for communication and not for localization, the number of APs in a building may be huge, but the existing infrastructure may still not be suitable for positioning. Several APs carrying redundant information for positioning purposes can be placed in the vicinity of each other, while in some other parts of the building there may be lack of APs. Therefore, it is important for the positioning accuracy point of view to figure out the sufficient AP density and the best possible AP configuration.

Our paper focuses on the investigation of the AP topology in the context of indoor positioning, based on a newly derived Cramér-Rao Lower Bound (CRLB)-based criterion. AP deployment for positioning purposes has previously been studied, e.g., in [6]–[10]. In [6], the impact of AP placement and number of APs for the location accuracy is studied based on experiments in two buildings. The conclusions are however drawn based on configurations with very small number of APs. A novel approach to place the APs is presented in [7]. The results are based on one floor in one particular building and demand 200 measurements for each FP, that can be unpractical and expensive for larger buildings. In [8], the idea is to place the APs in a way, where at least three APs are always heard while keeping the number of deployed APs as low as possible. The results presented in [8] are based on simulations only, as well as in [9], where another optimization method for AP placement is proposed. In [10], both AP coverage for communication purposes and FP differences are taken into account in a network design, but again the results are validated with very few APs and using simulations only.

The questions raised for the AP density and configuration set-up based on the CRLB are very rarely studied in the literature to the best of the Authors' knowledge. CRLB has previously been characterized for the RSS-based PL positioning approach in [11]. In [12], the CRLB has been derived for received signal strength difference (RSSD) based FP. Indeed, the CRLB has been derived for the RSS-based positioning in sensor networks in [13] and further used to optimize the placement of anchor nodes in [14], without comparisons with real measurement data. In [15], the influence of geometry and quantity of APs is studied shortly based on the derived CRLB for RSS measurements in WLAN network, but again, the studies are based on simulations and limited number of APs only.

The main difference between our paper and the publications [6]–[15] is that our purpose is to define and prove a theoretical

limit, that can be used both as a tool to understand the limits of an existing AP deployment and to provide specifications for AP placement if a WLAN network can be built for positioning purposes. With the presented criterion it can be seen what is the best possible positioning accuracy, with the current AP topology, and also to predict what it can be if the number of APs is increased. In our paper, the proposed CRLB-based limit is verified based on real-field data gathering, that consist of indoor measurements in eight different multi-floor buildings in two countries. Both FP and PL positioning methods are addressed.

II. POSITIONING ALGORITHMS

There are two well-known approaches in RSS-based positioning: FP [4], [5] and PL approaches [16], [17].

A. Fingerprint (FP) approach

The FP approach is a map matching technique, where a radiomap database (i.e., fingerprints, FPs) is created in the training phase, and in the estimation phase only the information in FPs is used together with the real-time observed RSSs to estimate the user position [1]. The radiomap FPs are in our research formed as $(x_i, y_i, z_i, P_{i,ap})$, where $P_{i,ap}$ denotes the observed RSS (in dBm) of apth AP in the ith FP and x_i, y_i, z_i are the 3D coordinates for ith FP. Here, $i = 1, ..., N_{fp}$, where N_{fp} denotes the total number of FPs in the radiomap. In our study, the radiomap consists of square box FPs. This means that the grid resolution is fixed (e.g., 1 m x 1 m) and all data samples that occur in this area are mapped to the same FP.

When comparing observed RSS levels (O_{ap}) by the MS with the RSS levels in the FPs, user location is calculated using Bayesian estimation with Gaussian likelihood $\mathcal{L}_i$ [4]:

$$\mathcal{L}_i = \sum_{ap=1}^{N} log\left(\frac{1}{\sqrt{2\pi\sigma_{ap}^2}} e^{\left(-\frac{(O_{ap}-P_{i,ap})^2}{2\sigma_{ap}^2}\right)} \right). \quad (1)$$

Here, σ_{ap}^2 represents a noise variance, that contains both shadowing effect and measurement error effect and N denotes the number of APs that are detected both in the current measurement and in the FP. If no prior knowledge about σ_{ap}^2 is known, then a same fixed value can be used for all APs. Some examples of typical indoor values for AP variances can be found for example in [18], [19]. The use of nearest neighbor (NN) averaging is also possible: N_n FPs $\hat{i}_n$ with maximum Gaussian likelihoods $\mathcal{L}_{\hat{i}_n}$ are chosen, and the user location is calculated as a mean over N_n nearest neighbor positions.

B. Path-Loss (PL) approach

Alternatively to the FP, a PL model can be used. The most common PL model is the one-slope model $P_{i,ap} = P_{T_{ap}} - 10\, n_{ap}\, log_{10}\, d_{i,ap} + \eta_{i,ap}$ [20], where n_{ap} is the PL coefficient and $P_{T_{ap}}$ the transmit power for the apth AP. Indeed, $d_{i,ap}$ denotes the range between the apth AP and the ith FP (i.e., $d_{i,ap} = \|\mathbf{x}_i - \mathbf{x}_{ap}\|$). $\eta_{i,ap}$ is a Gaussian distributed noise factor, that has standard deviation (std) σ_{ap} and zero mean.

The one-slope PL model in matrix form is [21]

$$\mathbf{P_{ap}} = \mathbf{H_{ap}}\, \mathbf{\Theta_{ap}^{T}} + \mathbf{n}, \quad (2)$$

where $\mathbf{n}$ represents a Gaussian distributed noise vector of size $N_F \times 1$, Θ_{ap} includes the unknown PL parameters for apth AP (i.e., $\Theta_{ap} = [n_{ap}\, P_{T_{ap}}]$), $\mathbf{P_{ap}}$ contains RSSs for apth AP (i.e., $\mathbf{P_{ap}} = [P_{1,ap}\, P_{2,ap}\, ... \, P_{N_F,ap}]$), $\mathbf{T}$ is transpose operator, and

$$\mathbf{H_{ap}} = \begin{bmatrix} 1 & -10log_{10}d_{1,ap} \\ & ... \\ 1 & -10log_{10}d_{N_F,ap} \end{bmatrix}. \quad (3)$$

Eq. 3 is possible to be solved by using classical deconvolution approaches, for example Least Squares [21]. The AP location estimate x_{ap}, y_{ap}, z_{ap} is obtained through brute-force approach [22].

The training stage in PL approaches provides estimates of the AP positions and the PL parameters n_{ap} and $P_{T_{ap}}$, based on the same radiomap than in FP approach. In the estimation phase, the MS location is computed using the PL parameters and the observed RSS by the MS. The main motivation of PL method is the amount of stored parameters and their ability to offer statistical solutions for large areas. With PL approaches, we can save up to 11 times in the database size [21].

III. PROPOSED CRLB-BASED ANALYSIS

The CRLB derives a lower bound on the variance of any unbiased estimator of an unknown parameter [23]. CRLB has been derived to RSS-based measurements in [13], [15]. Similarly, if the estimate of the user location is $\hat{\phi} = (\hat{x}\ \hat{y}\ \hat{z})^T$, its covariance matrix is

$$Cov_\phi(\hat{\phi}) = \begin{bmatrix} \sigma_{\hat{x}}^2 & \sigma_{\hat{x}\hat{y}} & \sigma_{\hat{x}\hat{z}} \\ \sigma_{\hat{y}\hat{x}} & \sigma_{\hat{y}}^2 & \sigma_{\hat{y}\hat{z}} \\ \sigma_{\hat{z}\hat{x}} & \sigma_{\hat{z}\hat{y}} & \sigma_{\hat{z}}^2 \end{bmatrix} \quad (4)$$

We know that $Cov_\phi(\hat{\phi}) \geq \{I(\phi)\}^{-1}$ [23], where $I(\phi)$ is the Fisher matrix:

$$I(\phi) = E\left[\left(\frac{\partial ln\, p(x;\phi)}{\partial \phi} \right)^2 \right] = -E\left[\left(\frac{\partial^2 ln\, p(x;\theta)}{\partial^2 \theta} \right) \right]. \quad (5)$$

Here, the likelihood function $p(x;\phi)$ denotes the probability density function (pdf) of observations $x;\phi$ and expectation operation E is taken with respect to $p(x;\phi)$. Further on, by using Eqs. 4 and 5, the Fisher information matrix $I(\phi)$ can be denoted as

$$I(\phi) = - \begin{bmatrix} \frac{\partial^2 p(x;\phi)}{\partial^2 x} & \frac{\partial^2 p(x;\phi)}{\partial x \partial y} & \frac{\partial^2 p(x;\phi)}{\partial x \partial z} \\ \frac{\partial^2 p(x;\phi)}{\partial y \partial x} & \frac{\partial^2 p(x;\phi)}{\partial^2 y} & \frac{\partial^2 p(x;\phi)}{\partial y \partial z} \\ \frac{\partial^2 p(x;\phi)}{\partial z \partial x} & \frac{\partial^2 p(x;\phi)}{\partial z \partial y} & \frac{\partial^2 p(x;\phi)}{\partial^2 z} \end{bmatrix}. \quad (6)$$

The used pdf in this paper, taking into account the joint power (i.e., sum over all hearable APs), is

$$p(x;\phi) = \mathcal{L}_i = \sum_{ap=1}^{N_{AP}} \frac{1}{\sqrt{2\pi\sigma_{ap}^2}} e^{\frac{\left(-10n_{ap}\log_{10}\left(\frac{d}{d_{i,ap}}\right)\right)^2}{2\sigma_{ap}^2}}, \quad (7)$$

where d is the distance between the unknown MS location (x, y, z) and apth AP location. Using Eq. 7 into Eq. 6,

TABLE I
MEASUREMENT SCENARIOS.

	Building	Floor area [m^2]	Number of floors	N_{ap}	N_{user}	N_{fp}	Location	Measurement device
A	University, building 1	9500	4	309	158	1476	Tampere (Finland)	Windows
B	University, building 2	14000	3	353	176	584	Tampere (Finland)	Windows
C	Office, building 1	4900	9	333	850	624	Berlin (Germany)	Nexus
D	Office, building 2	3600	7	994	143	844	Tampere (Finland)	Nexus
E	Shopping mall 1	48000	6	405	520	1633	Berlin (Germany)	Nexus
F	Shopping mall 2	22000	6	326	205	1789	Tampere (Finland)	Windows
G	Shopping mall 3	28000	3	503	776	306	Berlin (Germany)	Nexus
H	Shopping mall 4	19000	3	69	215	274	Tampere (Finland)	Windows

TABLE II
MEASUREMENT RESULTS.

Building	CRLB [m]	FP (std) [m]	PL (std) [m]	AP density per m^2
A	1.18	7.94	15.78	0.0082
B	1.49	17.04	17.41	0.0083
C	1.45	7.22	10.37	0.0131
D	0.66	6.49	5.75	0.0395
E	1.86	12.36	17.47	0.0016
F	2.32	18.08	28.17	0.0024
G	2.83	15.30	29.65	0.0068
H	10.03	31.23	32.93	0.0012

the diagonal elements of Eq. 6 (ξ being one of the x, y, z coordinates) are

$$\frac{\partial^2 \ ln \ p(\xi; \phi)}{\partial^2 \xi} = \sum_{ap=1}^{N_{AP}} \rho \ \frac{(\xi - \xi_{ap})^2}{d^4}, \qquad (8)$$

where $\rho = (\frac{10 n_{ap}}{\sigma_{ap} \ln 10})^2$.

A. Network topology optimization for positioning purposes

Further on, the CRLB can be utilized to compute an optimal AP density in a building, when the building AP topology is flexible. The proposed steps to this process are following:

1) Generate randomly allocated APs inside a 3D building, according to certain rules (e.g., circular, rectangular, uniform, or according to known topology).
2) Generate the training data with randomly allocated measurement points and their associated RSS according to the PL model in Eq. 2
3) Generate random user tracks within the considered 3D building, e.g., via random walk model.
4) Based on the training data generated at Steps 1-3, and Eq. 8, compute the CRLB achievable in each generated scenario.
5) Choose the configuration (e.g., number of APs per building area) that gives the lowest average CRLB, under a sufficient number of Monte Carlo simulations (here, 10000).

B. Measurement-based Verification of the proposed CRLB-based criterion

In this Section, we verify through measurement-based results that the CRLB can be used to estimate the expected RSS-based positioning accuracy according to the AP density and AP topology in a building. Both FP and PL approaches are included. We assume that the PL coefficient n_{ap} is constant for the apth AP. The noise std σ_{ap} for each AP can be obtained from the measurements. The measurement samples were gathered in four shopping malls, two office buildings and two university buildings, i.e., all together eight multifloor buildings in Berlin, Germany and in Tampere, Finland. Two different tablets (an Android Nexus tablet and a Windows tablet) were used in the data gathering for both training and estimation phases. The collection was done manually utilizing HERE indoor maps, which were included in the tablets. The data samples, that formed the user tracks, were collected separately. All user tracks include measurements from several floors in each building. In one building, only one device was used, i.e., the training data and estimation data were always collected with same tablet. All buildings and their main characteristics are detailed in Table I. Since an AP stands for a MAC address, it may happen that more than one APs are located at the same position (e.g., as it is the case with transmitters supporting multiple BSSID).

Table II shows the CRLB and std of the positioning error (calculated in 3D) for both FP and PL method for all buildings. Also the AP density is included. When examining the Table II, it can be seen that the FP performs slightly better than the PL method and is closer to the CRLB in most cases, as expected. The only exception is for building D, where also the AP density is clearly higher than in the other buildings. In buildings A-D, the CRLB is at most 1.5 meters and the positioning results for FP are between 6-8 meters, except for building B. The reason for the lower results in building B may be in the AP configuration or in more challenging environment with inner courts. The smaller AP density for buildings E-H clearly increases both the CRLB and the positioning errors. Especially with building H, where the AP density is very small and most of the APs are located in one floor only, even the CRLB is 10 m. Based on the results shown in Table II, it can be concluded that the state-of-the-art approaches that reach sub 3 m positioning accuracy may be in limited conditions with fully gathered data, not truly in multi-floor environment. In a building with several floors and especially with incomplete data (e.g., building H), even the CRLB with unfiltered data rarely reaches sub 3 m accuracy. Additional
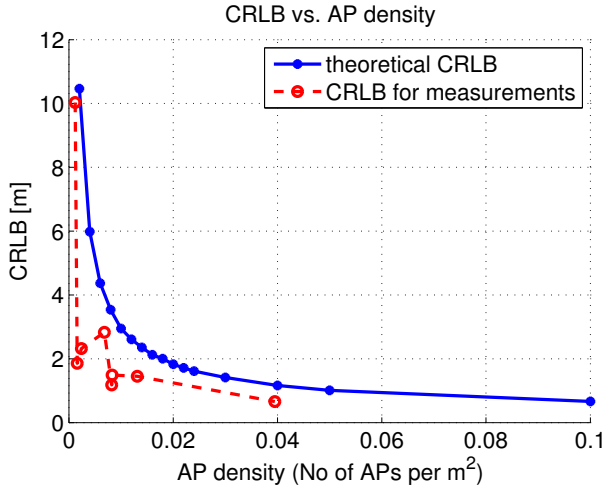
Fig. 1. CRLB vs. AP density both for a simulated building and real measurements (all buildings included). For simulated building, 10000 random points and 100 user measurements with random building size.

Fig. 2. Illustration of the Voronoi polygon areas between the estimated AP locations. Building C, floor 4.

filtering and sensor integration may indeed decrease the error. Also, according to [24], it is possible that an algorithm obtains better results than CRLB in the case of a biased estimator.

IV. SIMULATIONS AND MEASUREMENT-BASED RESULTS

A. Measurements-based results

In this Section, we will give an example of the use of CRLB for finding out a sufficient AP density for the best possible positioning results, using a 2D simulation model (one floor only). The building size is a m $\times$ b m, where both a and b are varied randomly between 50-150. Also both AP locations and user locations are randomly chosen inside the building (i.e., uniform distribution), but the AP density is fixed. Fig. 1 shows the CRLB vs. AP density for both a simulated building and for the measurements. Because of the randomizing, the results for simulated building are calculated over 10000 iterations and 100 random user measurements. For the real measurements, the AP density is calculated as an average over all floors. As it can be seen in Fig. 1, the curves for CRLB vs. AP density for the simulated case and for the measurements are very close to each other. It can be also seen in Fig. 1 that exactly two meter accuracy is achieved with AP density $0.018/m^2$ (i.e., by placing an AP for about every 7.5 m). Indeed, we can achieve sub-meter accuracy by placing an AP for every $\sqrt{10} \approx 3$ m, but placing them closer than this won't bring much benefit. This is also intuitively clear.

B. AP density choice in flexible network topologies

Naturally not only the AP density but also the AP placements are important from the positioning accuracy point of view. Therefore, we calculated an average Voronoi area between the estimated AP locations to illustrate the effect of AP deployment. One example showing the Voronoi polygons for building C at 4th floor can be seen in 2. The polygons are drawn only within the building limits, i.e., the polygons outside the building area are not taken into account. Red circles
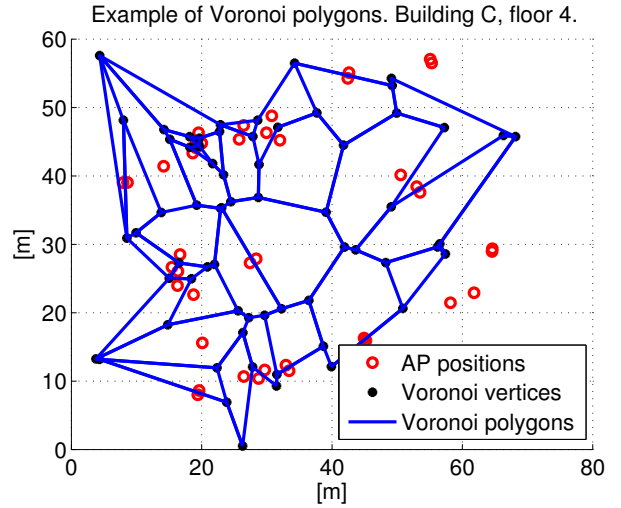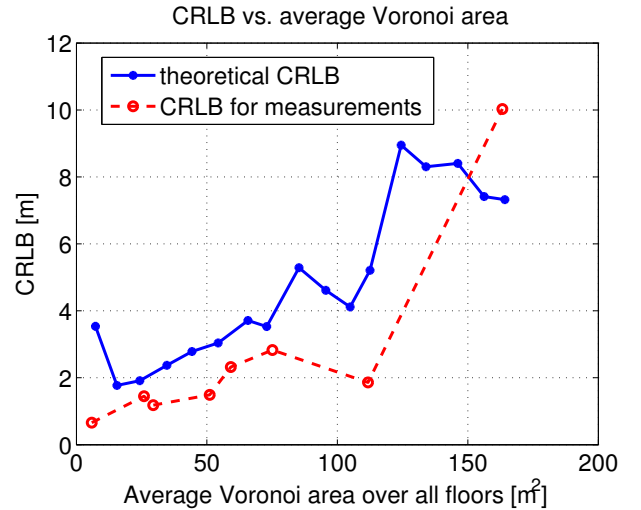

Fig. 3. CRLB vs. average Voronoi area over all floors both for a simulated building and real measurements (all buildings included). For simulated building, 10000 random points and 100 user measurements with random building size.

represent the AP locations, black dots Voronoi vertices, and blue lines determine the area of the polygon specified by the Voronoi vertices. The average Voronoi area is the average area of blue polygons.

Fig. 3 presents an average Voronoi area between the estimated AP locations for both simulated building and for the real measurements, within the building limits. As it can be seen, both theoretical (simulated) and real measurements follow the same trend: small Voronoi area corresponds to small CRLB, and higher Voronoi area to higher CRLB. The results in Fig. 3 verify that the CRLB-based criterion takes into account also the AP placements, not only AP density, and it is a powerful tool to predict the best possible positioning results for a particular AP deployment.

V. CONCLUSION

In this paper, we shown how a CRLB-based criterion can be used to estimate the expected accuracy bound in WLAN-networks with predefined topology or to find out the best AP density for a certain target of positioning accuracy, in a network designed for positioning purposes. We have proved the suitability of the CRLB criterion with measurement-based results, with both FP and PL approaches. We have explained how to use the CRLB and we have shown that that the CRLB-based criterion takes into account also the AP placements, not only AP density. The results we have presented here provide more insight for designing an efficient WLAN-based positioning environment and for evaluating existing WLAN AP topologies in the context of positioning accuracy.

ACKNOWLEDGMENT

REFERENCES

[1] S. H. Fang and T. N. Lin, *Accurate Indoor Location Estimation by Incorporating the Importance of Access Points in Wireless Local Area Networks*, Proc. of GLOBECOM, pp. 1-5, Dec 2010.

[2] G. Seco-Granados et al., *Challenges in Indoor GNSS: Unveiling its core features in signal processing*, IEEE Signal Process. Mag., vol. 29(2), pp. 108-131, Mar 2012.

[3] *IEEE Standard for Information technology-Telecommunications and Information Exchange Between Systems Local and Metropolitan Area Networks - Specific Requirements Part 11: Wireless LAN Medium Access Control (MAC) and Physical Layer (PHY) Specifications*, IEEE Std. 802.11-2012, 2012.

[4] V. Honkavirta et al., *A Comparative Survey of WLAN Location finger-printing Methods*, Proc. of WPNC, pp. 243-251, 2009.

[5] K. Kaemarungsi and P. Krishnamurthy, *Modeling of indoor positioning systems based on location fingerprinting*, Proc. of IEEE INFOCOM, Hong Kong, pp. 1012-1022, 2004.

[6] O. Baala et al., *The Impact of AP Placement in WLAN-Based Indoor Positioning System*, Proc. of ICN, Mar 2009.

[7] S.-H. Fang and T.-N. Lin, *A Novel Access Point Placement Approach for WLAN-Based Location Systems*, Proc. of IEEE WCNC, pp. 1-4, Apr 2010.

[8] K. Farkas, A. Huszak and G. Godor, *Optimization of Wi-Fi Access Point Placement for Indoor Localization*, Informatics & IT Today (IIT), vol 1(1), Jul 2013.

[9] S. Zirari et al., *Wi-Fi Access Point Placement within Stand-alone, Hybrid and Combined Wireless Positioning System*, Proc. of ICCE, pp. 1-5, Aug 2012.

[10] Q. Chen et al., *Placement of Access Points for Indoor Wireless Coverage and Fingerprint-based Localization*, Proc. of IEEE HPCC/EUC, pp. 2253-2257, Nov 2013.

[11] M. B. Zeytinci et al., *Location estimation using RSS measurements with unknown path loss exponents*, EURASIP Journal on Wireless Comm. and Networking, 2013.

[12] AK. M. M. Hossain and S.Wee-Seng, *Cramer-Rao Bound Analysis of Localization Using Signal Strength Difference as Location Fingerprint*, Proc. of IEEE INFOCOM, pp. 1-9, San Diego, 2010.

[13] N. Patwari et al., *Relative Location Estimation in Wireless Sensor Networks*, IEEE Transact. on Sign. Proc., vol. 51(8), Aug 2003.

[14] A. E. C. Redondi and E. Amaldi, *Optimizing the placement of anchor nodes in RSS-based indoor localization systems*, Proc. of 12th Annual Mediterranean Ad Hoc Networking Workshop, pp. 8-13, Jun 2013.

[15] M. Stella, Ma Russo and D. Begusic, *RF Localization in Indoor Environment*, in Radioengineering, vol 21(2), pp. 557-567, Jun 2012.

[16] P. Bahl and V. Padmanabhan, *RADAR: An in-building rf-based user location and tracking system*, Proc. of IEEE INFOCOM, pp. 775-784, Mar 2000.

[17] L. Bruno, M. Khider and P. Robertson, *On-line training of the path-loss model in Bayesian WLAN indoor positioning*, Proc. of IPIN, Oct 2013.

[18] E.S. Lohan, K. Koski, J. Talvitie and L. Ukkonen, *WLAN and RFID propagation channels for hybrid indoor positioning*, Proc. of IEEE ICL-GNSS, Helsinki, Finland, Jun 2014.

[19] E.S. Lohan et al., *Received Signal Strength models for WLAN and BLE-based indoor positioning in multi-floor buildings*, Proc. of IEEE ICL-GNSS, Gothenburg, Sweden, Jun 2015.

[20] H. Nurminen et al., *Statistical Path Loss Parameter Estimation and Positioning Using RSS Measurements in Indoor Wireless Networks*, Proc. of IPIN, Nov 2012.

[21] S. Shrestha, J. Talvitie and E. S. Lohan, *Deconvolution-based indoor localization with WLAN signals and unknown access point locations*, Proc. of ICL-GNSS, Jun 2013.

[22] Y. Cho et al., *Improved Wi-Fi AP position estimation using regression based approach*, Proc. of IPIN, Nov 2012.

[23] S. M. Kay, *Fundamentals of Statistical Signal Processing: Estimation Theory*. Prentice Hall.

[24] Reza Zekavat, R. Michael Buehrer, *Handbook of Position Location: Theory, Practice and Advances*. Wiley-IEEE Press (2011).